

Giant Electric Field Tuning of Magnetism in Novel Multiferroic FeGaB/Lead Zinc Niobate–Lead Titanate (PZN-PT) Heterostructures

By Jing Lou, Ming Liu, David Reed, Yuhang Ren, and Nian X. Sun*

Multiferroic composite materials consisting of both a magnetic phase and a ferroelectric phase are of great current interest, as they offer the possibility of magnetoelectric (ME) coupling, that is, electric field manipulation of magnetic properties (converse ME effect) or vice versa (direct ME effect),^[1–4] and have led to many novel multiferroic devices.^[5–12] One important series of such multiferroic devices is constituted by electrostatically tunable microwave multiferroic signal processing devices, including tunable resonators,^[9] phase shifters,^[10] and tunable filters.^[11,12] Compared to conventional tunable microwave magnetic devices, which are tuned by magnetic fields, these electrostatically tunable microwave multiferroic devices are much more energy efficient, less noisy, compact, and lightweight.

ME effects can be realized in multiferroic composites through a strain/stress-mediated interaction,^[1–5,7–14] which enables effective energy transfer between electric and magnetic fields and leads to important new functionalities and devices. Strong ME coupling is critical for multiferroic devices; however, it has been difficult to achieve at microwave frequencies, leading to a very limited tunability in electrostatically tunable microwave multiferroic devices. The demonstrated tunable range of most of these devices has been very limited, with a frequency tunability of $\Delta f < 150$ MHz and a low tunable magnetic field of $\Delta H < 50$ Oe^[9–12] ($1 \text{ Oe} \approx 79.6 \text{ A m}^{-1}$). This is mainly due to the large loss tangents at microwave frequencies of the two constituent phases, that is, the ferroelectric phase and, particularly, the magnetic phase, which is less resistive. The ME coupling strength in multiferroic composites is determined by many factors, such as the properties of the two constituent phases, the interface between them, the mode of ME coupling, and the orientation of the magnetic and electric fields. As a result, layered multiferroic heterostructures with magnetic thin films provide great opportunities for achieving strong ME coupling at microwave frequencies, owing to minimized charge leakage paths and low loss tangents associated with magnetic thin films. It is also desirable for the magnetic phase in the multiferroic composites to have a narrow ferromagnetic resonance (FMR)

linewidth and a large piezomagnetic coefficient ($d\lambda/dH$), that is, a large saturation magnetostriction constant (λ_s) and a low saturation magnetic field (H_s). However, such magnetic materials have not been readily available.

Very recently, we have reported a new class of metallic magnetic FeGaB films that has a high λ_s of ca. 70 ppm, a low H_s of ca. 20 Oe, and a narrow FMR linewidth of ca. 16 Oe at X-band (ca. 9.6 GHz).^[15] The maximum piezomagnetic coefficient of the FeGaB films is about 7 ppm Oe^{-1} , which is much higher than those of other well-known magnetostrictive materials used in multiferroic composites, such as Terfenol-D (Tb–Dy–Fe),^[16] Galfenol (Fe–Ga),^[17] and Metglas (FeBSiC),^[18] as shown in Figure 1. The combination of narrow FMR linewidth and high piezomagnetic coefficient makes these FeGaB films excellent candidates for the magnetic material in microwave multiferroic composites.^[19,20]

Single-crystal ferroelectrics such as lead magnesium niobate–lead titanate (PMN-PT)^[21] and lead zinc niobate–lead titanate (PZN-PT)^[22] having giant piezoelectric coefficients and low loss tangents are desired for microwave multiferroic composites as well. In particular, (011)-cut PMN-PT and PZN-PT single-crystal slabs have anisotropic piezoelectric coefficients d_{31} and d_{32} when poled along their [011] crystalline direction. For example, (011)-cut PZN-PT single crystals with 6% lead titanate have high anisotropic piezoelectric coefficients $d_{31} = -3000 \text{ pC N}^{-1}$ and $d_{32} = 1100 \text{ pC N}^{-1}$.^[22] The giant anisotropic piezoelectric coefficients of the PZN-PT single crystal provide great opportunities for generating a large in-plane magnetic anisotropic field and

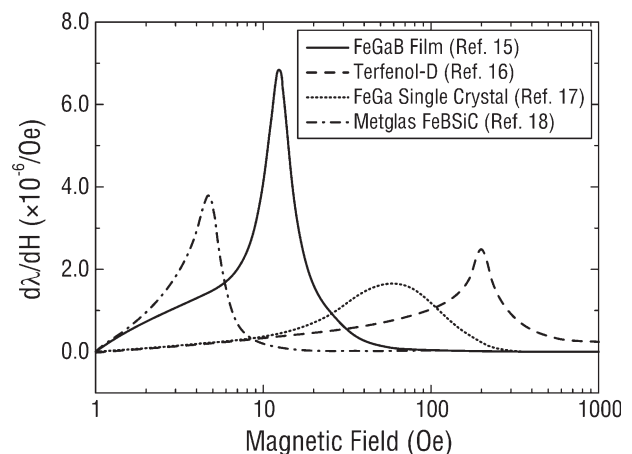


Figure 1. Piezomagnetic coefficients ($d\lambda/dH$) of different types of magnetostrictive alloys.

[*] Prof. N. X. Sun, J. Lou, M. Liu, D. Reed
Department of Electrical and Computer Engineering
Northeastern University
Boston, MA 02115 (USA)
E-mail: nian@ece.neu.edu
Prof. Y. H. Ren
Department of Physics and Astronomy
Hunter College, City University of New York
New York, NY 10065 (USA)

DOI: 10.1002/adma.200901131

therefore large frequency tunability in multiferroic composites.^[20]

In this Communication, we report on novel FeGaB/PZN-PT heterostructures that exhibit a record high electrostatically tunable FMR frequency range of 5.82 GHz or $f_{\max}/f_{\min} = 4.3$, and a giant electrostatically induced magnetic anisotropy field of ca. 750 Oe at both dc and microwave frequencies. This corresponds to a large mean ME coupling coefficient of $94 \text{ Oe} \cdot \text{cm} \cdot \text{kV}^{-1}$ and a giant mean electrostatically tunable frequency coefficient of $970 \text{ MHz} \cdot \text{cm} \cdot \text{kV}^{-1}$. Specifically, at the phase transition region of the PZN-PT single crystal, a colossal ME coupling coefficient of $2365 \text{ Oe} \cdot \text{cm} \cdot \text{kV}^{-1}$ and a giant electrostatically tunable frequency coefficient of $15 \text{ GHz} \cdot \text{cm} \cdot \text{kV}^{-1}$ are achieved. These parameters are about 1–3 orders of magnitude higher than published values.^[9–14,19,20] The FeGaB/PZN-PT multiferroic heterostructures with giant electrostatically tunable frequencies and magnetic anisotropy fields provide great opportunities for electrostatically tunable microwave signal processing devices.

Multiferroic heterostructures of FeGaB/PZN-PT were made by direct deposition of 100 nm FeGaB films using a magnetron sputtering method (see the Experimental section) onto PZN-PT single crystal slabs, as schematically shown in Figure 2. The FeGaB film had a magnetic easy axis that was induced during deposition by a bias magnetic field, which was oriented along the in-plane [001] direction of the PZN-PT single crystal to ensure maximum frequency tunability. Electric fields were applied across the thickness direction of the PZN-PT single crystal in order to utilize its high anisotropic piezoelectric coefficients d_{31} and d_{32} , which are also shown in Figure 2.

The field-sweep FMR spectra of the FeGaB/PZN-PT multiferroic heterostructure under different electric fields are shown in Figure 3. The external magnetic field was applied parallel to the in-plane [01 $\bar{1}$] direction of the PZN-PT single crystal, and was swept between 0 and 1400 Oe. Clearly, the FMR spectra changed dramatically with the external electric field, indicating a giant ME coupling in the FeGaB/PZN-PT heterostructure. The FMR field (the external magnetic field at which the power absorption spectrum dI/dH crosses zero, i.e., maximum power absorption) shifted from 1172 to 898 Oe on changing the external electric field from -2 to 5.8 kV cm^{-1} . A sudden change of the FMR field from 898 to 425 Oe occurred at electric fields between 5.8 and 6 kV cm^{-1} . Such a dramatic change of the FMR field within a very narrow electric field range is closely related to the phase transition

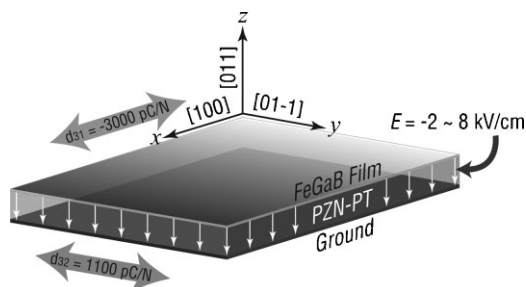


Figure 2. Scheme showing the structure of the FeGaB/PZN-PT multiferroic heterostructure. The coordinate system shows the crystalline directions of the PZN-PT single crystal.

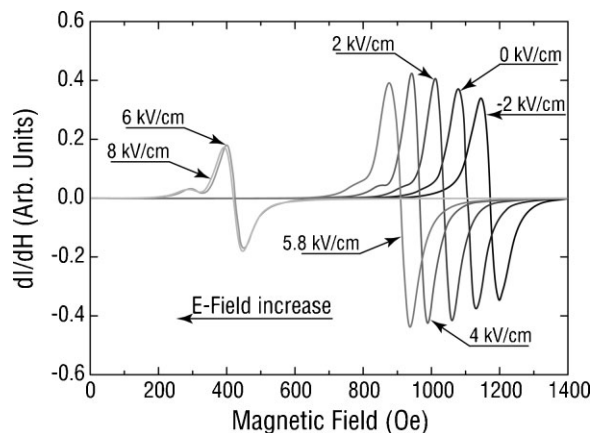


Figure 3. Electric field dependence of the in-plane field-sweep FMR spectra of the FeGaB/PZN-PT multiferroic heterostructure measured at ca. 9.6 GHz.

from the rhombohedral to the tetragonal phase in the PZN-PT single crystal, which has been reported previously.^[22] The FMR field barely changed at electric fields higher than 6 kV cm^{-1} , which was also consistent with the strain–electric field relation of the PZN-PT single crystal.^[22] It is important to emphasize that the overall electric-field-induced FMR field change (also the total electrostatically induced magnetic anisotropy) is ca. 750 Oe, which is the largest value that has ever been reported, corresponding to a mean ME coupling coefficient $\alpha = \Delta H/\Delta E = 94 \text{ Oe} \cdot \text{cm} \cdot \text{kV}^{-1}$. Specifically, the ME coupling coefficient amounts to $2365 \text{ Oe} \cdot \text{cm} \cdot \text{kV}^{-1}$ at the phase transition region of the PZN-PT single crystal. Meanwhile, the FMR linewidth of the FeGaB film, which is a critical parameter for microwave magnetic materials, stays at $50 \pm 5 \text{ Oe}$ under different electric fields. The ratio between the total tunable magnetic field and the FMR linewidth is as high as ca. 1500%, indicating an excellent figure of merit for tunable microwave devices.

Very recently, Eerenstein et al. have reported a multiferroic epitaxial heterostructure of 40 nm $\text{La}_{0.67}\text{Sr}_{0.33}\text{MnO}_3$ (LSMO) on a 0.5 mm single-crystal BaTiO_3 (BTO) substrate,^[13] which showed a large ME coupling coefficient $\alpha = \mu_0 \Delta M/\Delta E = 2.3 \times 10^{-7} \text{ s} \cdot \text{m}^{-1}$ near the orthorhombic-to-rhombohedral phase transition region of the BaTiO_3 . It is interesting to note that the two ME coupling coefficients can be converted to the same units of seconds per meter. However, the two different methods of calculating ME coupling coefficients, that is, through $\alpha = \Delta H/\Delta E$ and $\alpha = \mu_0 \Delta M/\Delta E$, represent two different physical quantities. For the LSMO/BTO heterostructure, the ME coupling coefficient was calculated from $\alpha = \mu_0 \Delta M/\Delta E$, which represents the electric-field-induced magnetization change, whereas the ME coupling coefficient for the FeGaB/PZN-PT heterostructures in this work were calculated by $\alpha = \Delta H/\Delta E$, the effective induced magnetic field per unit electric field, which is the electric-field-induced effective magnetic field change.

It is worth mentioning that the other widely used ME coupling coefficient $\alpha = \Delta P/\Delta H$, which is the electric polarization change per unit magnetic field, also has the units, seconds per meter.^[7] It can be calculated from $\alpha = \varepsilon_0 \chi \Delta E/\Delta H$, where χ is the electric susceptibility of the ferroelectric phase, and ε_0 is the permittivity

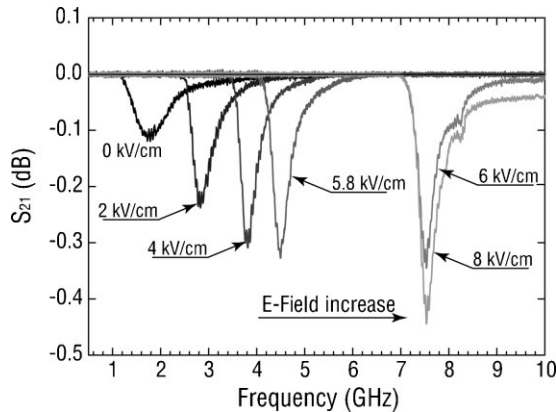


Figure 4. Electric field dependence of the transmission coefficient (S_{21}) spectra of the FeGaB/PZN-PT multiferroic heterostructure measured by network analyzer.

of vacuum. Although all four ME coupling coefficients, $\alpha = \mu_0 \Delta M / \Delta E$, $\alpha = \Delta H / \Delta E$, $\alpha = \Delta P / \Delta H$ and $\alpha = \Delta E / \Delta H$, have been used in the literature, they represent totally different physical quantities, making a meaningful comparison difficult.

The frequency-sweep FMR behavior of the FeGaB/PZN-PT multiferroic composite was also measured on a network analyzer, and is shown as the transmission coefficient S_{21} spectra in Figure 4. The main absorption peak in the S_{21} curves corresponds to the FMR, which shows strong electric field dependence, indicating a large tuning of the FMR frequency by electric fields. It is notable that the S_{21} spectra were measured without a bias magnetic field, indicating that such FeGaB/PZN-PT heterostructures can be operated under a self-biased condition over a wide range of operational frequency. The lowest FMR frequency is 1.75 GHz at zero electric field and the highest is 7.57 GHz at 6 or 8 kV cm⁻¹. The total electrostatically tunable FMR frequency range of 5.82 GHz is about two order of magnitude higher than reported values.^[9–12] This leads to an electrostatically tunable range of the FMR frequency of more than 2 octaves, or $f_{\max}/f_{\min} = 4.3$, corresponding to a mean tunable frequency per unit electric field of 970 MHz · cm · kV⁻¹, or 15 GHz · cm · kV⁻¹ at the phase transition region of the PZN-PT single crystal. The very large frequency tunability makes these FeGaB/PZN-PT multiferroic heterostructures attractive for electrostatically tunable microwave multiferroic devices.

The magnetic hysteresis loops of the FeGaB/PZN-PT multiferroic heterostructure were measured by vibrating-sample magnetometer (VSM) along the [100] direction of the PZN-PT single crystal under different electric fields, which also confirmed the large electric-field-induced effective magnetic anisotropy changes, as shown in Figure 5. Clearly, the electric-field-induced magnetic anisotropy field is the largest at electric fields of 6 and 8 kV cm⁻¹, and lowest at 0 kV cm⁻¹. The in-plane magnetic anisotropy fields at different electric fields can be estimated from the hysteresis loops, being ca. 20 Oe at 0 kV cm⁻¹ and ca. 700 Oe at 6 kV cm⁻¹ electric field. This leads to a ME coefficient of ca. 113 Oe · cm · kV⁻¹ at dc, which is close to the value obtained from the FMR measurements at microwave frequencies.

The electric-field-induced change in the in-plane magnetic anisotropy field, ΔH_{eff} , can be calculated by the piezoelectric and

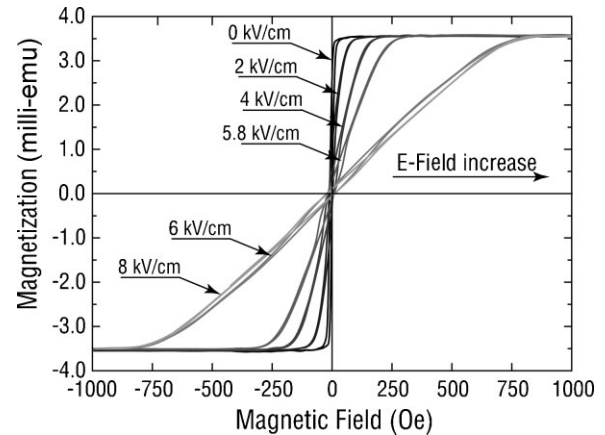


Figure 5. Magnetic hysteresis loops of the FeGaB/PZN-PT multiferroic heterostructure under different external electric fields measured by VSM.

inverse magnetoelastic equations. Since the thicknesses of the FeGaB film and electrode layers are much less than that of the PZN-PT single-crystal substrate, the FeGaB film experiences an in-plane stress induced by the piezoelectric strain of the PZN-PT single crystal, leading to an induced effective magnetic field of (cgs units)

$$\Delta H_{\text{eff}} = 3\lambda_s d_{\text{eff}} E Y / M_s \quad (1)$$

where Y is Young's modulus of the FeGaB film, d_{eff} is the effective piezoelectric coefficient, E is the applied electric field, and M_s is the saturation magnetization. Assuming a plane stress condition, d_{eff} can be calculated as

$$d_{\text{eff}} = \frac{\nu d_{32} + d_{31}}{1 - \nu^2} - \frac{\nu d_{31} + d_{32}}{1 - \nu^2} = \frac{d_{31} - d_{32}}{1 + \nu} \quad (2)$$

where ν is the Poisson ratio of the FeGaB film. Clearly, the anisotropic piezoelectric coefficients of the PZN-PT single crystal are desirable in achieving large electric-field-induced magnetic anisotropy fields. The magnetic anisotropy fields induced by ME coupling can therefore be estimated, with Young's modulus of about 55 GPa for the FeGaB film; they are listed in Table 1 together with measured ΔH_{eff} from field-sweep FMR measurements. The theoretical and experimental data show very good agreement.

Table 1. Calculated and measured electric-field-induced effective magnetic field ΔH_{eff} of the FeGaB/PZN-PT multiferroic heterostructure under different electric fields.

| Electric field [kV cm ⁻¹] | 0 | 2 | 4 | 5.8 | 6 | 8 |
|---|---|----|-----|-----|---------|---------|
| Calculated ΔH_{eff} [Oe] | 0 | 78 | 156 | 227 | 632 [a] | 640 [a] |
| Measured ΔH_{eff} [Oe] | 0 | 69 | 139 | 207 | 680 | 686 |

[a] These values are estimated from the strain–electric field curve [22] of the PZN-PT single crystal since its piezoelectric constant is no longer proportional to the electric field.

We describe the electric-field-induced shift of the FMR field or frequency by the Landau–Lifshitz equation of motion for the magnetization.^[23] The eigenfrequencies of the standing spin waves can be described by

$$\omega_k^2 = \gamma^2 \left(H_{dc} + \frac{2K_{\parallel}}{M_s} + \Delta H_{\text{eff}} + Dk^2 \right) \times \left(H_{dc} + \frac{2K_{\parallel}}{M_s} + 4\pi M_s - \frac{2K_{\perp}}{M_s} + \Delta H_{\text{eff}} + Dk^2 \right) \quad (3)$$

where H_{dc} is the external magnetic field, K_{\perp} and K_{\parallel} are the out-of-plane and in-plane uniaxial anisotropy constants, D is the spin stiffness, and k is the spin wave vector.

It is obvious from Equations 1–3 that the FMR frequency can be tuned by both magnetic and electric fields. Hence we are able to estimate the FMR frequency of the FeGaB/PZN-PT multiferroic heterostructure under different magnetic and electric bias fields. In order to better understand the dual tunability of the FeGaB/PZN-PT multiferroic, a three-dimensional (3D) chart for the FMR frequency versus the electric and magnetic fields was constructed and is shown in Figure 6. Clearly, the estimated FMR frequencies match the experimental data very well.

It is notable that the interface of the multiferroic heterostructures plays a crucial role in determining the ME coupling strength, as well as the resonance modes (or eigenfrequencies) of FeGaB films. In addition to the FMR field shift, we notice a significant change of the line shape in Figure 3 when the electric field is increased. The spectra become more asymmetric with increasing electric field. A relatively weak absorption peak at the lower field side of the main mode can be deconvoluted from the FMR spectra in Figure 3, which is attributed to the first-order standing spin wave mode along the FeGaB film thickness direction. The standing spin wave mode disturbs the main

resonance line and introduces an additional contribution to the FMR linewidth as well as the asymmetric line shape. Such a double resonance feature can also be clearly observed in Figure 4, particularly at a high applied electric field. The appearance of the first-order standing spin wave testifies to the fact that there is a free boundary condition on one of the FeGaB film surfaces, while on the other surface, that is, the interface, the spins are gradually pinned by the increasing stress induced by the deformation of the PZN-PT single crystal, since in uniform thin films FMR selection rules allow only excitations with a net magnetic moment. In other words, asymmetric boundary conditions at the FeGaB/PZN-PT interface are realized by electrostatically induced ME coupling in the FeGaB/PZN-PT heterostructure, which is responsible for the excitation of standing spin waves.

In conclusion, novel FeGaB/PZN-PT multiferroic heterostructures have been synthesized and characterized. A large electric-field-induced effective magnetic anisotropy field of ca. 750 Oe with a narrow FMR linewidth of ca. 50 Oe was observed at X-band in the FeGaB/PZN-PT heterostructure, which was consistent with the observed effective magnetic field change at dc. The FeGaB/PZN-PT heterostructure exhibited a large mean ME coupling coefficient $\alpha = \Delta H/\Delta E = 94 \text{ Oe} \cdot \text{cm} \cdot \text{kV}^{-1}$, and a giant ME coupling coefficient of $2365 \text{ Oe} \cdot \text{cm} \cdot \text{kV}^{-1}$ at the electric-field-induced phase transition region of the PZN-PT single crystal. The heterostructures also showed a large electric-field-tunable FMR frequency range between 1.75 and 7.57 GHz under zero bias magnetic field, corresponding to a mean tunable frequency per unit electric field of about $970 \text{ MHz} \cdot \text{cm} \cdot \text{kV}^{-1}$. The FMR frequency tunability was as high as $15 \text{ GHz} \cdot \text{cm} \cdot \text{kV}^{-1}$ at the PZN-PT phase transition region. The giant tunable magnetic field and FMR frequency of the FeGaB/PZN-PT multiferroic heterostructures make them promising candidates for wide-band electrostatically tunable microwave devices.

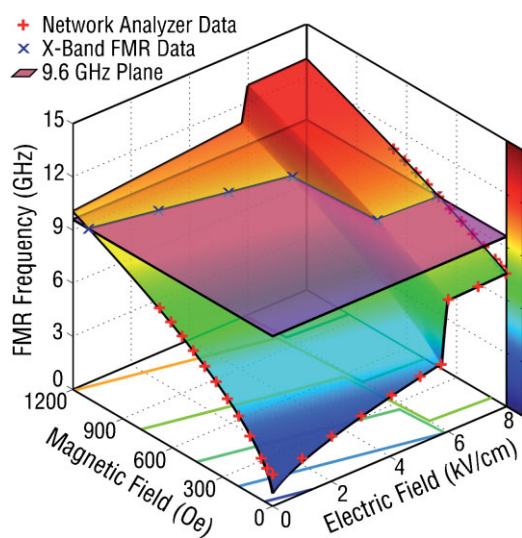


Figure 6. 3D plot showing the FMR frequency of the FeGaB/PZN-PT multiferroic heterostructure as a function of external magnetic and electric bias fields.

Experimental

Materials and Methods: Multiferroic heterostructures of FeGaB/PZN-PT were fabricated by direct deposition of bilayers of $\text{Ni}_{80}\text{Fe}_{20}$ (Permalloy)/FeGaB films onto commercially available (011)-cut and [011]-poled PZN–6%PT single-crystal slabs with a thickness of 0.5 mm. The Permalloy layer, which had a thickness of ca. 5 nm, was used as a seed layer for achieving better magnetic softness and narrow FMR linewidth [24]. The FeGaB films used in this work have a saturation magnetization of ca. 10 kG (1 kG = 0.1 T), an initial relative permeability μ_i of ca. 400, and a saturation magnetostriction constant of ca. 60 ppm.

An electron paramagnetic resonance spectrometer operating at X-band (ca. 9.6 GHz) with a TE_{102} microwave cavity was used to characterize the microwave performance of the FeGaB/PZN-PT heterostructures. The dc magnetic field was applied in the film plane and parallel to the [011] direction of the PZN-PT single crystal while the magnetic component of the microwave field was parallel to the [100] direction of the PZN-PT single crystal.

The FeGaB/PZN-PT multiferroic heterostructures were loaded onto a coplanar waveguide (CPW) that was connected to the two ports of a vector network analyzer to analyze the electrostatically tunable FMR frequencies in the frequency domain. External bias magnetic fields ranging from zero to 700 Oe were applied parallel to the wave propagation direction of the CPW, and parallel to the [011] direction of the PZN-PT to achieve strong coupling.

Acknowledgements

This work is financially supported by NSF awards 0824008 and 0746810 and ONR awards N000140710761 and N000140810526.

Received: April 2, 2009

Published online: August 5, 2009

-
- [1] M. Fiebig, *J. Phys. D: Appl. Phys.* **2005**, *38*, R123.
[2] N. Spaldin, M. Fiebig, *Science* **2005**, *309*, 391.
[3] W. Eerenstein, N. D. Mathur, J. F. Scott, *Nature* **2006**, *442*, 759.
[4] C. W. Nan, M. I. Bichurin, S. X. Dong, D. Viehland, G. Srinivasan, *J. Appl. Phys.* **2008**, *103*, 031101.
[5] J. Zhai, Z. Xing, S. X. Dong, J. F. Li, D. Viehland, *Appl. Phys. Lett.* **2006**, *88*, 062510.
[6] J. F. Scott, *Nat. Mater.* **2007**, *6*, 256.
[7] C. Israel, N. D. Mathur, J. F. Scott, *Nat. Mater.* **2008**, *7*, 94.
[8] J. Lou, D. Reed, M. Liu, N. X. Sun, *Appl. Phys. Lett.* **2009**, *94*, 112508.
[9] Y. K. Fetisov, G. Srinivasana, *Appl. Phys. Lett.* **2006**, *88*, 143503.
[10] A. Ustinov, G. Srinivasan, B. A. Kalinikos, *Appl. Phys. Lett.* **2007**, *90*, 031913.
[11] C. Pettiford, S. Dasgupta, J. Lou, S. D. Yoon, N. X. Sun, *IEEE Trans. Magn.* **2007**, *43*, 3343.
[12] A. S. Tatarenko, V. Gheevarghese, G. Srinivasan, *Electron. Lett.* **2006**, *42*, 540.
[13] W. Eerenstein, M. Wiora, J. L. Prieto, J. F. Scott, N. D. Mathur, *Nat. Mater.* **2007**, *6*, 348.
[14] M. Liu, O. Obi, J. Lou, S. Stoute, J. Y. Huang, Z. Cai, K. S. Ziemer, N. X. Sun, *Appl. Phys. Lett.* **2008**, *92*, 152504.
[15] J. Lou, R. E. Insignares, Z. Cai, K. S. Ziemer, M. Liu, N. X. Sun, *Appl. Phys. Lett.* **2007**, *91*, 182504.
[16] M. B. Moffett, A. E. Clark, M. Wun-Fogle, J. Linberg, J. P. Teter, E. A. McLaughlin, *J. Acoust. Soc. Am.* **1991**, *89*, 1448.
[17] A. E. Clark, M. Wun-Fogle, J. B. Restorff, T. A. Lograsso, J. R. Cullen, *IEEE Trans. Magn.* **2001**, *37*, 2678.
[18] S. X. Dong, J. Zhai, J. Li, D. Viehland, *Appl. Phys. Lett.* **2006**, *89*, 252904.
[19] C. Pettiford, J. Lou, L. Russell, N. X. Sun, *Appl. Phys. Lett.* **2007**, *92*, 122506.
[20] J. Lou, D. Reed, C. Pettiford, M. Liu, P. Han, S. Dong, N. X. Sun, *Appl. Phys. Lett.* **2008**, *92*, 262502.
[21] P. Han, W. Yan, J. Tian, X. Huang, H. Pan, *Appl. Phys. Lett.* **2005**, *86*, 052902.
[22] L. C. Lim, K. K. Rajan, J. Jin, *IEEE Trans. Ultrason. Ferroelect. Freq. Control* **2007**, *54*, 2474.
[23] L. Landau, E. Lifshitz, *Phys. Z. Sowjetunion* **1935**, *8*, 153.
[24] S. X. Wang, N. X. Sun, M. Yamaguchi, S. Yabukami, *Nature* **2000**, *407*, 150.
-